

Published in: Phys. Rev. E **92**, 052106 (2015).

Identifying the order of a quantum phase transition by means of Wehrl entropy in phase-space

Octavio Castaños*

*Instituto de Ciencias Nucleares, Universidad Nacional Autónoma de México,
Apdo. Postal 70-543, 04510, DF, Mexico*

Manuel Calixto†

*Departamento de Matemática Aplicada,
Facultad de Ciencias, Universidad de Granada,
Fuentenueva s/n, 18071 Granada, Spain.*

Francisco Pérez-Bernal‡

*Departamento de Física Aplicada, Facultad de Ciencias Experimentales,
Universidad de Huelva, Campus del Carmen,
Avda. de las Fuerzas Armadas s/n, 21071 Huelva, Spain.*

Elvira Romera§

*Departamento de Física Atómica, Molecular y Nuclear and
Instituto Carlos I de Física Teórica y Computacional,
Universidad de Granada, Fuentenueva s/n, 18071 Granada, Spain.*

Abstract

We propose a method to identify the order of a Quantum Phase Transition by using area measures of the ground state in phase space. We illustrate our proposal by analyzing the well known example of the Quantum Cusp, and four different paradigmatic boson models: Dicke, Lipkin-Meshkov-Glick, interacting boson model, and vibron model.

*Electronic address: ocasta@nucleares.unam.mx

†Electronic address: calixto@ugr.es

‡Electronic address: francisco.perez@dfaie.uhu.es

§Electronic address: eromera@ugr.es

I. INTRODUCTION

The extremely relevant concept of phase transition in Thermodynamics has been extended in later times to encompass novel situations. In particular, two main aspects have been recently addressed: the study of mesoscopic systems and of quantum systems at zero temperature. In the first case, the finite system size modifies and smooths phase transition effects. In the second case a tiny modification of certain Hamiltonian parameter or parameters (control parameters) induces an abrupt change in the ground state of the quantum system and Quantum Phase Transitions (QPTs) appear as an effect of quantum fluctuations at the critical value of the control parameter [1]. QPTs strictly occur in infinite systems, though QPT precursors are present in finite systems. In fact, bosonic models allow to study both aforementioned aspects: finite-size effects and zero temperature QPTs. Recent reviews on this subject are [2–4].

QPTs occurring in finite-size systems can be characterized by the disappearance of the gap between the ground and the first excited state energies in the mean field or thermodynamic limit (infinite system size). The QPT is a first order phase transition if a level crossing occurs and a continuous transition if there are no crossings (except in the limit value) [5]. The Landau theory holds in the models addressed in this presentation, and within this theory the Ehrenfest classification of QPTs is valid. In this case, the order of a QPT is assigned on the basis of discontinuities in derivatives of the potential of the system at the thermodynamic limit [3, 4].

The assignment of the order of a phase transitions in finite-size systems using a numerical treatment to compute finite differences of the system energy functional can be a cumbersome task. In order to overcome this problem, different approaches have been proposed. Cejnar *et al.* have used the study of nonhermitian degeneracies near critical points to classify the order of QPTs [5]. Alternative characterizations are based in the connection between geometric Berry phases and QPTs in the case of the XY Ising model [6, 7] and in the overlap between two ground state wave functions for different values of the control parameter (fidelity susceptibility concept) [8–10]. In addition, many efforts have been devoted to characterize QPTs in terms of information theoretic measures of delocalization (see [11–14] and references therein) and quantum information tools, e. g. using entanglement entropy measures (see e.g. [15] for the Dicke model and [16, 17] for the vibron model).

In this work we propose an alternative way to reckon the order of a QPT by using the Wehrl entropy in the phase-space (coherent state or Bargmann) representation of quantum states ψ provided by the Husimi function Q_ψ , which is defined as the squared overlap between ψ and an arbitrary coherent state.

The Husimi function has been widely used in quantum physics, mainly in quantum optics. For example, the time evolution of coherent states of light in a Kerr medium is visualized by measuring Q_ψ by cavity state tomography, observing quantum collapses and revivals, and confirming the non-classical properties of the transient states [18]. Moreover, the zeros of this phase-space quasi-probability distribution have been used as an indicator of the regular or chaotic behavior in quantum maps for a variety of quantum problems: molecular [19] and atomic [20] systems, the kicked top [21], quantum billiards [22], or condensed matter systems [23] (see also [24, 25] and references therein). They have also been considered as an indicator of metal-insulator [26] and topological-band insulator [27] phase transitions, as well as of QPTs in Bose Einstein condensates [10] and in the Dicke [28, 29], vibron [17], and Lipkin-Meshkov-Glick (LMG) models [30].

To identify the order of a QPT we suggest to observe the singular behavior of the Wehrl entropy, W_ψ , of the Husimi function, Q_ψ , near the critical point as the system size increases. The Wehrl entropy, is defined in Sec. III as a function of the Hamiltonian control parameter(s) and the system's size. For harmonic oscillators, Lieb proved in [31] the Wehrl's conjecture [32] stating that W_ψ attains its minimum (maximum area) when ψ is an ordinary (Heisenberg-Weyl) coherent state. This proof has been recently extended by Lieb and Solovej to $SU(2)$ spin- j systems [33]. We observe that W_ψ is maximum at the critical point of a first-order QPT, and this maximum is narrower as the system size increases. However, for second-order QPTs, the Wehrl entropy displays a step function behavior at the critical point, and again the transition is sharper for larger system sizes. We shall confirm this behavior for five models: Quantum Cusp, Dicke, LMG, a one-dimensional realization of the interacting boson model (IBM-LMG), and the 2D limit of the vibron model (2DVM).

We have chosen the Cusp model as a prototypical case, because this is probably the best known catastrophe example, describing the bifurcation of a critical point with a quartic potential. Its quantum version [34] has been used to illustrate the effects associated with criticality as a prior step to deal with more involved physical situations [3, 34–36]. In addition to the Cusp model, we present results for four different realizations of bosonic

systems. The LMG model is a simple model, originally introduced for the description of nuclear systems as an exactly-solvable toy model to assess the quality of different approximations [37]. This ubiquitous model still receives a major attention, further stimulated by its recent experimental realization [38, 39]. The study of the ground state quantum phase transitions for this model can be traced back to the seminal articles of Gilmore and Feng [40, 41]. The Dicke model is a quantum-optical model that describes the interaction of a radiation field with N two-level atoms [42]. This model has recently renewed interest [43–46], partly because a tunable matter-radiation interaction is a keynote ingredient for the study of quantum critical effects [15, 47, 48] and partly because the model phase transition has been observed experimentally [49]. The interacting boson model (IBM) was introduced by Arima and Iachello to describe the structure of low energy states of even-even medium and heavy nuclei [50]. For the sake of simplicity, we use the IBM-LMG, a simplified version of the model built with scalar bosons [51]. Finally, the vibron model was also proposed by Iachello to describe the rovibrational structure of molecules [52] and the 2DVM was introduced [53] to model molecular bending dynamics (e.g. see Ref. [54] and references therein). The 2DVM is the simplest two-level model which still retains a non-trivial angular momentum quantum number and it has been used as a playground to illustrate ground state and excited state QPTs features in bosonic models [55, 56].

We proceed to present the Hamiltonian of the five different addressed models, defining the Wehrl entropy as functions of the moments of the Husimi function Q_ψ , and the results obtained in the first and second order critical points of the different models considered. A brief introduction to the main results on Schwinger boson realizations, coherent states, and energy surfaces used in the paper can be found in App. A.

II. SELECTED MODELS

We give a brief outline of the five models we use to illustrate the characterization of QPT critical points by means of the Wehrl entropy.

The first model is the one dimensional quantum cusp Hamiltonian [3, 34–36]

$$\hat{H} = \frac{K^2 \hat{p}^2}{2} + V_c(\hat{x}) , \quad (1)$$

where $V_c(\hat{x}) = \frac{1}{4}\hat{x}^4 + \frac{u}{2}\hat{x}^2 + v\hat{x}$ is the cusp potential, with control parameters u and v and

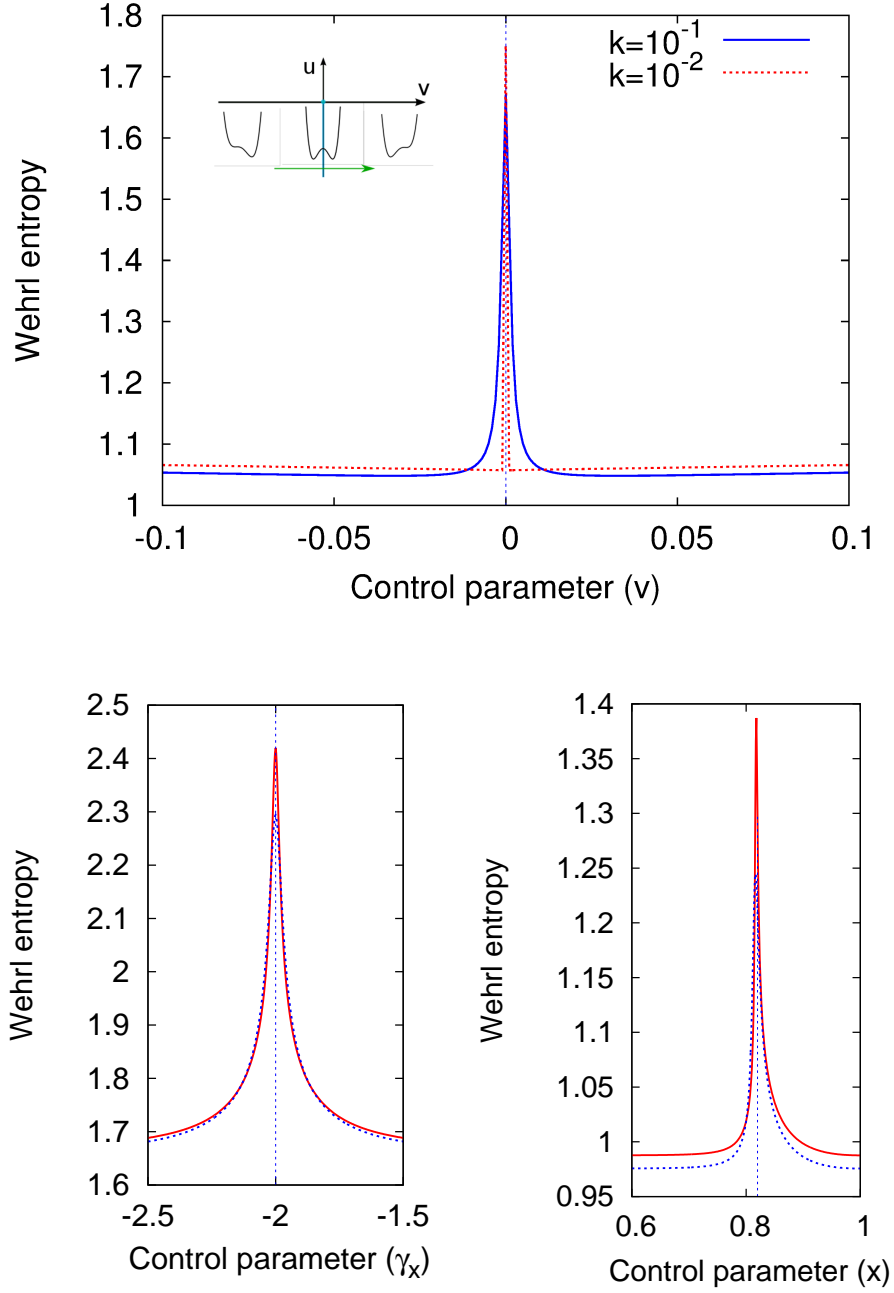


FIG. 1: (Color online) First order QPTs: Wehrl entropy W_ψ of the Husimi function for the ground state. Top panel: cusp model for $k = 10^{-1}$ (blue, solid) and 10^{-2} (red, dashed), along the straight line $u = -1$ with critical point $v_c = 0$. Bottom left: LMG model for $N = 20$ (blue, dashed) and 40 (red, solid), along the straight line $\gamma_x = -\gamma_y - 4$ with critical point $\gamma_{xc} = -2$. Bottom right: IBM-LMG model for $N = 80$ (red, solid) and $N = 40$ (blue, dashed), for the straight line $y = \frac{1}{\sqrt{2}}$ with critical point $x_c = 0.82$. Critical points are marked with vertical blue dotted lines.

a classicality constant $K = \frac{\hbar}{\sqrt{M}}$, combining \hbar and the mass parameter M (see [35]). The smaller the value of K the closer the system is to the classical limit. The mass parameter M can be fixed to unity without loss of generality. In order to obtain energies and eigenstates for the quantum Cusp, we have recast Hamiltonian (1) in second quantization, using harmonic oscillator creation and annihilation operators, and diagonalized the resulting matrix with a careful assessment of convergence. The ground state quantum phase transitions associated with the cusp have been studied using Catastrophe Theory and Ehrenfest's classification [3] and making use of entanglement singularities [36]. It is well known that there is a first order quantum phase transition line when the control parameter v changes sign for negative u values, and a second order transition point for $v = 0$ and u moving from negative to positive values. In this work we will consider two trajectories: (i) for $u = -1$ and $v \in [-0.2, 0.2]$ with a first order critical point at $v_c = 0$, and (ii) for $v = 0$ and $u \in [-1, 1]$ with a second order critical point at $u_c = 0$.

The Dicke model is an important model in quantum optics that describes a bosonic field interacting with an ensemble of N two-level atoms with level-splitting ω_0 . The Hamiltonian is given by

$$\hat{H} = \omega_0 \hat{J}_z + \omega a^\dagger a + \frac{\lambda}{\sqrt{2j}} (a^\dagger + a)(\hat{J}_+ + \hat{J}_-) , \quad (2)$$

where \hat{J}_z , \hat{J}_\pm are angular momentum operators for a pseudospin of length $j = N/2$, and a and a^\dagger are the bosonic operators of a single-mode field with frequency ω . There is a second order QPT at a critical value of the atom-field coupling strength $\lambda_c = \frac{1}{2}\sqrt{\omega\omega_0}$, with two phases: the normal phase ($\lambda < \lambda_c$) and the superradiant phase ($\lambda > \lambda_c$) [57, 58]. Several tools for the identification of its QPTs have been proposed: by means of entanglement [15], information measures (see [11, 13] and references therein) and in terms of fidelity [59], inverse participation ratio, the Wehrl entropy and the zeros of the Husimi function and marginals [28, 29, 60].

We will also deal with an interacting fermion-fermion model, the LMG model [37]. In the quasispin formalism, except for a constant term, the Hamiltonian for N interacting spins can be written as

$$\frac{\hat{H}}{2\omega j} = \frac{\hat{J}_z}{j} + \frac{\gamma_x}{j(2j-1)} \hat{J}_x^2 + \frac{\gamma_y}{j(2j-1)} \hat{J}_y^2 , \quad (3)$$

where γ_x and γ_y are control parameters. We would like to point out that the total angular momentum $J^2 = j(j+1)$ and the number of particles $N = 2j$ are conserved, and \hat{H}

commutes with the parity operator for fixed j . Ground state quantum phase transitions for this model have been characterized using the continuous unitary transformation technique [61], investigating singularities in the complex plane (exceptional points) [62], and from a semiclassical perspective [63]. A complete classification of the critical points has been accomplished using the catastrophe formalism [64, 65]. We will study the first and second order QPTs given by the trajectories $\gamma_x = -\gamma_y - 4$ and $\gamma_x = -\gamma_y + 2$ in the phase diagram [65]. A characterization of QPTs in the LMG model has recently been performed in terms of Rényi-Wehrl entropies, zeros of the Husimi function and fidelity and fidelity susceptibility concepts [30].

In the case of the characterization of the phase diagram associated with the IBM it is important to emphasize the pioneer works on shape phase transitions on nuclei [66], that anticipated the detailed construction of the phase diagram of the interacting boson model using either catastrophe theory [66, 67], the Landau theory of phase transitions [68, 69], or excited levels repulsion and crossing [70]. In the present work we use the IBM-LMG, a simplified one dimensional model, which shows first and second order QPTs, having the same energy surface as the Q-consistent interacting boson model Hamiltonian [51]. In this case the Hamiltonian is

$$\hat{H} = x\hat{n}_t - \frac{1-x}{N}\hat{Q}^y\hat{Q}^y, \quad (4)$$

with $\hat{n}_t = t^\dagger t$ and $\hat{Q}^y = s^\dagger t + t^\dagger s + y t^\dagger t$ are expressed in terms of two species of scalar bosons s and t , and the Hamiltonian has two control parameters x and y . The total number of bosons $N = \hat{n}_s + \hat{n}_t$ is a conserved quantity. For $y = 0$ there is an isolated point of second order phase transition as a function of x with a critical value $x_c = 0.8$. For $y > 0$ the phase transition is of first order and, to illustrate this case, we have chosen the value $y = 1/\sqrt{2}$, with a critical control parameter $x_c = 0.82$.

Finally, the 2DVM is a model which describes a system containing a dipole degree of freedom constrained to planar motion. Elementary excitations are (creation and annihilation) 2D Cartesian τ -bosons and a scalar σ -boson. The second order ground state quantum phase transition in this model has been studied in Ref. [56] using the essential Hamiltonian

$$\hat{H} = (1 - \xi)\hat{n} + \xi \frac{N(N+1) - \hat{W}^2}{N-1}, \quad (5)$$

where the (constant) quantum number N labels the totally symmetric representation $[N]$ of $U(3)$, $\hat{n} = \tau_+^\dagger \tau_+ + \tau_-^\dagger \tau_-$ is the number operator of vector bosons, and $\hat{W}^2 = (\hat{D}_+ \hat{D}_- +$

$\hat{D}_- \hat{D}_+)/2 + \hat{l}^2$. The operators $\hat{D}_+ = \sqrt{2}(\tau_+^\dagger \sigma - \sigma^\dagger \tau_-)$ and $\hat{D}_- = \sqrt{2}(-\tau_-^\dagger \sigma + \sigma^\dagger \tau_+)$ are dipole operators, and $\hat{l} = \tau_+^\dagger \tau_+ - \tau_-^\dagger \tau_-$ is the angular momentum operator. This model has a single control parameter $0 \leq \xi \leq 1$ and the second order QPT takes place at a critical value $\xi_c = 0.2$ [56]. Several procedures have been used to identify the ground state QPT in this model: entanglement entropies [16], Rényi entropies [12], the Wehrl entropy, and the inverse participation ratio of the Husimi function [71].

III. WEHRL'S ENTROPY AND GROUND STATE QPTS

We have numerically diagonalized the Hamiltonians of the five models for two different values of the system size N in an interval of control parameters containing a critical point (either first- or second-order). Given the expansion $|\psi\rangle = \sum_n c_n |n\rangle$ of the ground state in a basis $\{|n\rangle, n \in I\}$ (I denotes a set of quantum indices) with coefficients c_n depending on the control parameters and the system's size N , and given the expansions of coherent states $|\zeta\rangle$ in the corresponding basis (see App. A), we can compute the Husimi function $Q_\psi(\zeta) = |\langle \zeta | \psi \rangle|^2$ and the Wehrl entropy

$$W_\psi = - \int Q_\psi(\zeta) \ln[Q_\psi(\zeta)] d\mu(\zeta), \quad (6)$$

where we are generically denoting by $d\mu(\zeta)$ the measure in each phase space with points labeled by ζ . Note that W_ψ is a function of the control parameters and the system size N . We discuss typical (minimum) values of W_ψ for each model, which are attained when the ground state ψ is coherent itself, and Wehrl entropy values of parity-adapted (Schrödinger cat) coherent states [72, 73], which usually appear in second-order QPTs [16, 17, 28, 30, 44, 45]. *Cusp:* in the top panel of Figs. 1 and 2 we plot W_ψ as a function of the control parameters u and v for two trajectories and two values of the classicality constant K . The first order case is for trajectory $u = -1$, depicted in Fig. 1, with a critical control parameter $v_c = 0$. In this case it is immediately apparent a sudden growth of Wehrl entropy of the ground state at the critical point $v_c = 0$. The entropy growth is sharper as K decreases. The ground state is approximately a coherent state for $v \neq 0$ and a cat-like state for $v = 0$. Indeed, as conjectured by Wehrl [32] and proved by Lieb [31], any Glauber coherent state $|\psi\rangle = |\beta\rangle$ has a minimum Wehrl entropy of $W_\psi = 1$. It has also been shown [16, 28–30] that parity adapted coherent (Schrödinger cat) states, $|\psi\rangle \propto |\beta\rangle + |-\beta\rangle$, increase the minimum entropy

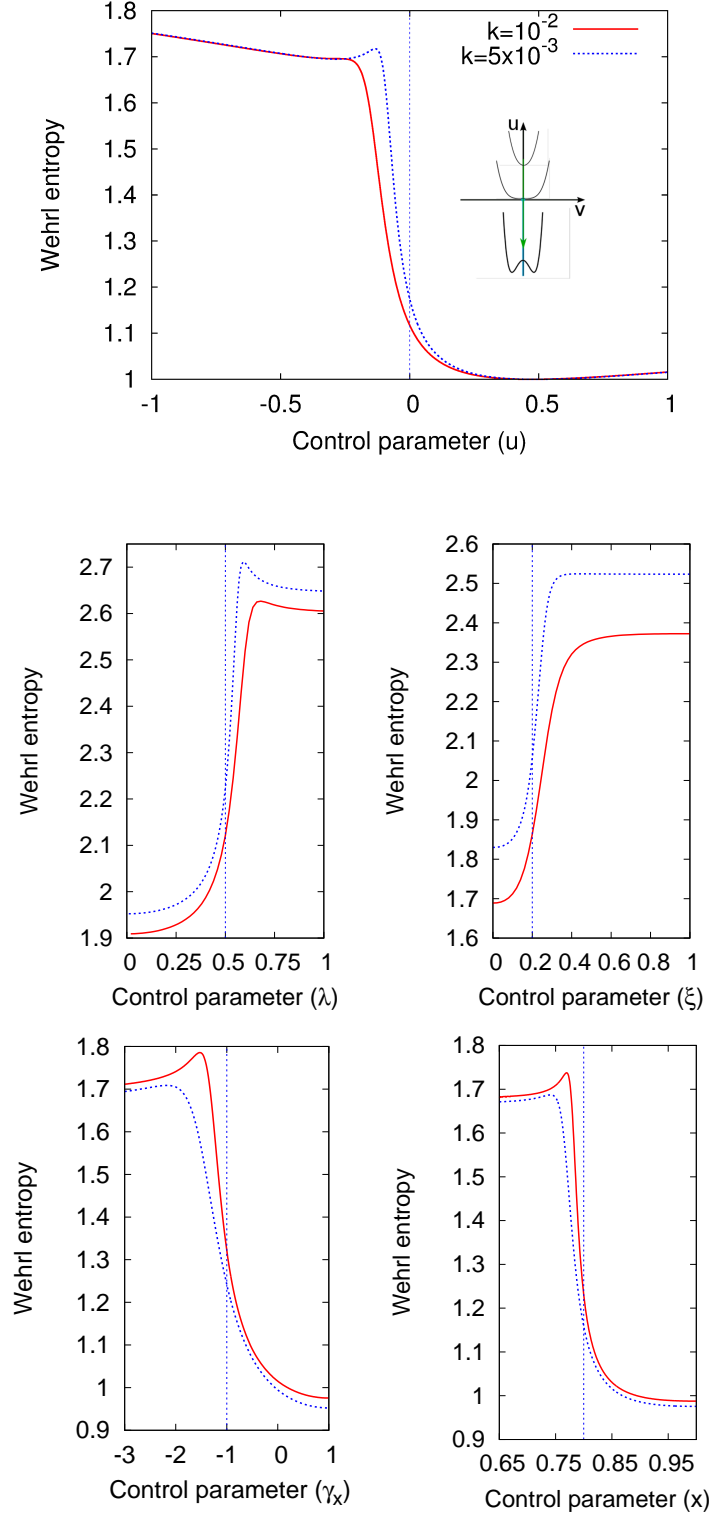


FIG. 2: (Color online) Second order QPTs: Wehrl entropy W_ψ of the Husimi function for the ground state. Top panel: cusp model for $K = 10^{-2}$ (red, solid) and 10^{-3} (blue, dashed), along the straight line $u = 0$ with critical point $v_c = 0$. Mid left panel: Dicke model for $N = 10$ (red, solid) and 20 (blue, dashed) with critical point $\lambda_c = 0.5$; mid right panel: 2DVM results for $N = 8$ (red, solid) and 16 (blue, dashed) with critical point $\xi_c = 0.2$. Bottom left panel: LMG model for $N = 20$ (blue, dashed) and 40 (red, solid), along the straight line $\gamma_x = -\gamma_y + 2$ with critical

by approximately $\ln(2)$ (for negligible overlap $\langle -\beta|\beta\rangle$). With this information, we infer that the ground state $|\psi\rangle$ is approximately a coherent state in the phase $u > 0$ and a cat-like state in the phase $u < 0$.

The second order QPT case is shown in Fig. 2, with $v = 0$ and critical control parameter $u_c = 0$. For the second trajectory, if we move from positive to negative values of u , we find in the top panel of Fig. 2 a sudden growth of W_ψ in the vicinity of the critical point $u_c = 0$ jumping from $W_\psi(u > 0) \simeq 1$ to $W_\psi(u < 0) \simeq 1 + \ln(2)$. The entropy growth is sharper as K decreases (classical limit).

Therefore, we would like to emphasize the utterly different entropic behavior of first- and second-order QPTs. In both cases we also plot an inset with the parameter trajectory and the evolution of the potential along it. We proceed to show that this Wehrl entropy behavior is shared by the rest of the considered models too, allowing a clear distinction between first and second order QPTs.

LMG: the LMG model has first and second order transitions depicted in the bottom left panels of Figs. 1 and 2, respectively. We plot W_ψ as a function of the control parameters γ_x and γ_y for the trajectories: $\gamma_y = -\gamma_x - 4$ (1^{st} order QPT at $\gamma_{xc} = -2$, bottom left panel Fig. 1) and $\gamma_y = -\gamma_x + 2$ (2^{nd} order QPT at $\gamma_{xc} = -1$, bottom left panel Fig. 2), for two values of the total number of particles N . We observe an entropic behavior completely similar to the Cusp model. The difference only lies on the particular entropy values. In fact, according to Lieb's conjecture [31, 33]), spin- j coherent states have a minimum Wehrl entropy of $W_\psi = \frac{2j}{2j+1}$, which tends to $W_\psi = 1$ in the thermodynamic limit $j \rightarrow \infty$. Cat-like states again increase the minimum entropy by approximately $\ln(2)$. The IBM-LMG model exhibits a similar behavior to the LMG model, as can be appreciated in the bottom right panel of Figs. 1 and 2.

Dicke: the Dicke model exhibits a 2nd-order QPT at the critical value of the control parameter $\lambda_c = 0.5$, when going from the normal ($\lambda < \lambda_c$) to the superradiant ($\lambda > \lambda_c$) phase. W_ψ captures this transition, as it can be seen in the mid left panel of Fig. 2, showing an entropy increase from $W_\psi \simeq 1 + \frac{N}{N+1}$ to $W_\psi \simeq 1 + \frac{N}{N+1} + \ln(2)$, with $N = 2j$ the number of atoms. As expected, the entropic growth at λ_c is sharper for higher N .

Vibron: the vibron model undergoes a 2nd-order (shape) QPT at $\xi_c = 0.2$, the critical point that marks a change between linear ($\xi < \xi_c$) and bent ($\xi > \xi_c$) phases [56]. In the mid right panel of Fig. 2 we plot the Wehrl entropy as a function of ξ for two values of the system's size

N (total number of bosons). As in the previous models, the 2nd-order QPT is characterized by a “step function” behavior of W_ψ near the critical point. In this case, we have conjectured [16] that minimum entropy $W_\psi = \frac{N(3+2N)}{(N+1)(N+2)}$ is attained for $U(3)$ coherent states. In the bent phase, the ground state $|\psi\rangle$ is a cat [16, 17, 71] and therefore $W_\psi \simeq \frac{N(3+2N)}{(N+1)(N+2)} + \ln(2)$.

IV. CONCLUDING REMARKS

In summary, we have numerically diagonalized the Hamiltonians of five models for several system’s sizes N in a given interval of control parameters that contains a critical point (either of first or second order). Given the expansion $|\psi\rangle = \sum_n c_n |n\rangle$ of the ground state in a basis $\{|n\rangle, n \in I\}$ (I denotes a set of quantum indices) with coefficients c_n depending on the control parameters and the system’s size N , and given the expansions of coherent states in the corresponding basis, we can compute the Husimi function Q_ψ and the Wehrl entropy W_ψ . In Figs. 1 and 2 we plot W_ψ as a function of a control parameter for different values of N .

From the obtained results it is clear that the Wehrl entropy behavior at the vicinities of the critical point is an efficient numerical way of distinguishing first order and continuous QPTs.

It is worth to emphasize that the present approach could imply an extra computational cost if compared to the search of nonanalyticities in the ground state energy functional. The present method makes use of the ground state wave functions for different values of the control parameter and it also requires the calculation of the overlap of the basis states with the coherent states. Though the need of ground state wavefunctions instead of ground state energies is computationally more exigent, the finer sensitivity of the present method largely offsets the extra computational cost. The second step, the overlap with coherent states, needs to be done only once with available analytic expressions (see App. A), therefore it does not constitute a significant computational burden. The proposed approach permits a clear determination of the character of a critical point using relatively small basis sets. On the contrary, even for large system sizes, the numerical determination with finite differences of the critical points character could remain ambiguous.

A similar sensitivity and computational cost could be attained with the fidelity susceptibility approach, that provides a clear determination of the critical point location, but with no

information of the transition order and with the additional hindrance of varying the control parameter in two different scales. Something similar happens with entanglement entropy measures, that are suitable to be applied to bipartite or multipartite systems, the critical point is clearly located but no precise information about the transition order is obtained.

Acknowledgments

We thank J. E. García Ramos for useful discussion. Work in University of Huelva was funded through MINECO grants FIS2011-28738-C02-02 and FIS2014-53448-C2-2-P and by Spanish Consolider-Ingenio 2010 (CPANCS2007-00042). Work in University of Granada was supported by the Spanish Projects: MINECO FIS2014-59386-P, and the Junta de Andalucía projects P12.FQM.1861 and FQM-381.

Appendix A: Schwinger boson realizations, coherent states and energy surfaces

a. Single mode radiation fields are described by harmonic oscillator creation a^\dagger and annihilation a operators in Fock space $\{|n\rangle = \frac{(a^\dagger)^n}{\sqrt{n!}}|0\rangle\}$, and the corresponding normalized coherent state (CS) is given by:

$$|\alpha\rangle = e^{-|\alpha|^2/2} e^{\alpha a^\dagger} |0\rangle = e^{-|\alpha|^2/2} \sum_{n=0}^{\infty} \frac{\alpha^n}{n!} |n\rangle, \quad (\text{A1})$$

where $\alpha = x + ip \in \mathbb{C}$ is given in terms of the quadratures x, p of the field. The phase space (Bargmann) representation of a given normalized state $|\psi\rangle = \sum_{n=0}^{\infty} c_n |n\rangle$ of the (single mode) radiation field is given by the Husimi function $Q_\psi(\alpha) = |\langle\alpha|\psi\rangle|^2$, which is normalized according to $\int_{\mathbb{R}^2} Q_\psi(\alpha) d\mu(\alpha) = 1$, with measure $d\mu(\alpha) = \frac{1}{\pi} d^2\alpha = \frac{1}{\pi} dx dp$.

b. Two-mode (a_1, a_2) boson condensates with $N = 2j$ particles are described in terms of SU(2) operators, whose Schwinger realization is

$$J_+ = a_2^\dagger a_1, \quad J_- = a_1^\dagger a_2, \quad J_z = \frac{1}{2}(a_2^\dagger a_2 - a_1^\dagger a_1). \quad (\text{A2})$$

In the case of the Dicke model, J_\pm, J_z represent collective operators for an ensemble of N two-level atoms. Spin- j coherent states (CSs) are written in terms of the Fock basis states $|n_1 = j - m; n_2 = j + m\rangle \equiv |j, m\rangle$ (with n_1 and n_2 the occupancy number of levels 1 and 2)

as:

$$\begin{aligned}
|\zeta\rangle &= \frac{1}{\sqrt{(2j)!}} \frac{(a_2^\dagger + \zeta a_1^\dagger)^{2j}}{(1 + |\zeta|^2)^j} |0\rangle \\
&= (1 + |\zeta|^2)^{-j} \sum_{m=-j}^j \binom{2j}{j+m}^{1/2} \zeta^{j+m} |j, m\rangle,
\end{aligned} \tag{A3}$$

where $\zeta = \tan(\theta/2)e^{-i\phi}$ is given in terms of the polar θ and azimuthal ϕ angles on the Riemann sphere. The phase-space representation of a normalized state $|\psi\rangle = \sum_{m=-j}^j c_m |j, m\rangle$ is now $Q_\psi(\zeta) = |\langle\zeta|\psi\rangle|^2$, which is normalized according to $\int_{\mathbb{S}^2} Q_\psi(\zeta) d\mu(\zeta) = 1$, with integration measure (solid angle) $d\mu(\zeta) = \frac{2j+1}{4\pi} \sin\theta d\theta d\phi$.

The IBM-LMG model, based on a scalar (s) and a pseudo-scalar (t) boson creation and annihilation operators has been written in terms of SU(2) operators (A2), with $s = a_1$ and $t = a_2$.

c. Three-mode (a_0, a_1, a_2) models (like the 2DVM) with N particles are described in terms of U(3) operators, whose Schwinger realization is $J_{jk} = a_j^\dagger a_k$, $j, k = 0, 1, 2$. U(3) coherent states, in the symmetric representation, are written in terms of the Fock basis states $|n_0 = N - n; n_1 = (n + l)/2; n_2 = (n - l)/2\rangle \equiv |N, n, l\rangle$ [with n_j the occupancy number of level $j = 0, 1, 2$ and $n = 0, \dots, N$ (the bending quantum number), $l = n - 2m$ (the 2D angular momentum), $m = 0, \dots, n$] as:

$$\begin{aligned}
|\zeta_1, \zeta_2\rangle &= \frac{1}{\sqrt{N!}} \frac{(a_0^\dagger + \zeta_1 a_1^\dagger + \zeta_2 a_2^\dagger)^N}{(1 + |\zeta_1|^2 + |\zeta_2|^2)^{N/2}} |0\rangle, \\
&= \sum_{n=0}^N \sum_{m=0}^n \frac{\{N! / [(N - n)!(n - m)!m!]\}^{1/2}}{(1 + |\zeta_1|^2 + |\zeta_2|^2)^{N/2}} \\
&\quad \times \zeta_1^{n-m} \zeta_2^m |N, n, l = n - 2m\rangle,
\end{aligned} \tag{A4}$$

with $\zeta_1, \zeta_2 \in \mathbb{C}$. The phase-space representation of a normalized state $|\psi\rangle = \sum_{n=0}^N \sum_{m=0}^n c_{nm} |N, n, l = n - 2m\rangle$ is now $Q_\psi(\zeta_1, \zeta_2) = |\langle\zeta_1, \zeta_2|\psi\rangle|^2$, which is normalized according to $\int_{\mathbb{R}^4} Q_\psi(\zeta_1, \zeta_2) d\mu(\zeta_1, \zeta_2) = 1$, where

$$d\mu(\zeta_1, \zeta_2) = \frac{(N+1)(N+2)}{\pi^2} \frac{d^2\zeta_1 d^2\zeta_2}{(1 + |\zeta_1|^2 + |\zeta_2|^2)^3}$$

is the integration measure on the complex projective (quotient) space $\mathbb{CP}^2 = \text{U}(3)/\text{U}(2) \times \text{U}(1)$ and $d^2\zeta_{1,2} \equiv d\text{Re}(\zeta_{1,2}) d\text{Im}(\zeta_{1,2})$ the usual Lebesgue measure on \mathbb{R}^2 .

The connection with our $U(3)$ construction to the 2DVM is $a_0 = \sigma$ and $a_{1,2}$ are the so called circular bosons: $\tau_{\pm} = \mp(\tau_x \mp i\tau_y)/\sqrt{2}$, respectively.

In order to make the article as self-contained as possible, let us also briefly recall the classical Hamiltonians or energy surfaces (the Hamiltonian operator expectation value in a coherent state) and their critical points for the selected models. The cusp model has already been discussed in section II.

For the Dicke model, using harmonic oscillator CSs (A1) for the field and spin- j CSs (A3) for the atoms, the energy surface turns out to be:

$$\langle \alpha, \zeta | \hat{H} | \alpha, \zeta \rangle = \omega |\alpha|^2 + j\omega_0 \frac{|\zeta|^2 - 1}{|\zeta|^2 + 1} + \lambda \sqrt{2j} \frac{4\Re(\alpha)\Re(\zeta)}{|\zeta|^2 + 1}. \quad (\text{A5})$$

Minimizing with respect to α and ζ gives the equilibrium points $\alpha_e = 0 = \zeta_e$ if $\lambda < \lambda_c$ (normal phase) and

$$\alpha_e = -\sqrt{2j} \sqrt{\frac{\omega_0}{\omega}} \frac{\lambda}{\lambda_c} \sqrt{1 - \frac{\lambda_c^4}{\lambda^4}}, \quad \zeta_e = \sqrt{\frac{\lambda^2 - \lambda_c^2}{\lambda^2 + \lambda_c^2}}, \quad (\text{A6})$$

if $\lambda \geq \lambda_c$ (superradiant phase). For the LMG model, the energy surface written in terms of $\zeta = \tan(\theta/2)e^{-i\phi}$ is:

$$\frac{\langle \zeta | \hat{H} | \zeta \rangle}{2\omega j} = -\cos\theta + \sin^2\theta \left(\frac{\gamma_x}{2} \cos^2\phi + \frac{\gamma_y}{2} \sin^2\phi \right). \quad (\text{A7})$$

The minimization process results in three phases for this system: 1) region $\gamma_x < -1$ with $\gamma_x < \gamma_y$, 2) region $\gamma_y < -1$ with $\gamma_y < \gamma_x$ and 3) region $\gamma_y > -1$ and $\gamma_x > -1$; for more information, like bifurcation sets associated with the absolute minimum of the energy surface, we address the reader to Ref. [65].

The analysis of the IBM-LMG case performed in [51] shows how for a two-mode coherent state $|\beta\rangle$ [the large N limit of $|\zeta\rangle$ in (A3), with $\zeta = \beta \in \mathbb{R}$], the resulting energy surface in the thermodynamic limit is

$$\begin{aligned} \frac{\langle \zeta | \hat{H} | \zeta \rangle}{N} &= \frac{\beta^2}{(1 + \beta^2)^2} \\ &\times \left\{ 5x - 4 + 4\beta y(x - 1) + \beta^2 [x + y^2(x - 1)] \right\}, \end{aligned} \quad (\text{A8})$$

that coincides with that of the Q-consistent IBM Hamiltonian [51]. If the control parameter $y = 0$ there is an isolated second order phase transition point as a function of the control parameter x with a critical value $x_c = 0.8$. If $y > 0$ and constant the phase transition is of

first order and minima coexistence occurs for the critical value $x_c = (4 + y^2)/(5 + y^2)$. In particular, the results shown for a first order phase transition in the bottom right panel of Fig. 1, with $y = 1/\sqrt{2}$, are equivalent to the results obtained in the IBM model in the case of a transition from a U(5) (spherical) to a SU(3) (axially symmetric) configuration in the Casten triangle [68].

Finally, for the 2DVM [56], due to the underlying (rotational) symmetries, one can restrict himself to particular U(3) CSs (A4) with $\zeta_1 = r/\sqrt{2} = -\zeta_2$, so that the energy surface turns out to be simply

$$\frac{\langle \zeta_1, \zeta_2 | \hat{H} | \zeta_1, \zeta_2 \rangle}{N} = (1 - \xi) \frac{r^2}{1 + r^2} + \xi \left(\frac{1 - r^2}{1 + r^2} \right)^2. \quad (\text{A9})$$

The minimization process results in two phase-shapes: 1) linear phase ($\xi \leq \xi_c = 1/5$), with ‘equilibrium radius’ $r_e = 0$ and 2) bent phase ($\xi > \xi_c$), with $r_e(\xi) = \sqrt{(5\xi - 1)/(3\xi + 1)}$.

-
- [1] L. D. Carr, *Understanding Quantum Phase Transitions* (Series in Condensed Matter Physics, CRC Press, Taylor & Francis Group., 2010).
 - [2] R. F. Casten, Prog. Part. Nucl. Phys. **62**, 183 (2009).
 - [3] P. Cejnar and J. Jolie, Prog. Part. Nucl. Phys. **62**, 210 (2009).
 - [4] P. Cejnar, J. Jolie, and R. F. Casten, Rev. Mod. Phys. **82**, 2155 (2010).
 - [5] P. Cejnar, S. Heinze, and M. Macek, Phys. Rev. Lett. **99**, 100601 (2007).
 - [6] A. C. M. Carollo and J. K. Pachos, Phys. Rev. Lett. **95**, 157203 (2005).
 - [7] S.-L. Zhu, Phys. Rev. Lett. **96**, 077206 (2006).
 - [8] P. Zanardi and N. Paunković, Phys. Rev. E **74**, 031123 (2006).
 - [9] S.-J. Gu, Int. J. Mod. Phys. B **24**, 4371 (2010).
 - [10] C. Pérez-Campos, J. R. González-Alonso, O. Castaños, and R. López-Peña, Ann. Phys. **325**, 325 (2010).
 - [11] A. Nagy and E. Romera, Physica A **391**, 3650 (2012).
 - [12] E. Romera, R. del Real, M. Calixto, S. Nagy, and A. Nagy, J. Math. Chem. **51**, 620 (2013).
 - [13] E. Romera, M. Calixto, and A. Nagy, Europhys. Lett. **97**, 20011 (2012).
 - [14] A. Nagy and E. Romera, Europhys. Lett. **109**, 60002 (2015).
 - [15] N. Lambert, C. Emary, and T. Brandes, Phys. Rev. A **71**, 053804 (2005).

- [16] M. Calixto, E. Romera, and R. del Real, J. Phys. A **45**, 365301 (2012).
- [17] M. Calixto and F. Pérez-Bernal, Phys. Rev. A **89**, 032126 (2014).
- [18] G. Kirchmair et al., Nature **495**, 205 (2013).
- [19] F. J. Arranz, Z. S. Safi, R. M. Benito, and F. Borondo, Eur. Phys. J. D **60**, 279 (2010).
- [20] P. A. Dando and S. Monteiro, J. Phys. B **27**, 2681 (1994).
- [21] S. Chaudhury et al., Nature **461**, 68 (2009).
- [22] J.-M. Tualle and A. Voros, Chaos Solitons Fract. **5**, 1085 (1995).
- [23] D. Weinmann, S. Kohler, G.-L. Ingold, and P. Hanggi, Ann. Phys. (Lpz.) **8**, SI277 (1999).
- [24] P. Leboeuf and A. Voros, J. Phys. A **23**, 1765 (1990).
- [25] F. J. Arranz, L. Seidel, C. G. Giralda, R. M. Benito, and F. Borondo, Phys. Rev. E **87**, 062901 (2013).
- [26] C. Aulbach et al., New Journal of Physics **6**, 70 (2004).
- [27] M. Calixto and E. Romera, Europhys. Lett. **109**, 40003 (2015).
- [28] R. del Real, M. Calixto, and E. Romera, Phys. Scripta **T153**, 014016 (2013).
- [29] E. Romera, R. del Real, and M. Calixto, Phys. Rev. A **85**, 053831 (2012).
- [30] E. Romera, M. Calixto, and O. Castaños, Phys. Scripta **89**, 095103 (2014).
- [31] E. H. Lieb, Comm. Math. Phys. **62**, 35 (1978).
- [32] A. Wehrl, Rep. Math. Phys. **16**, 353 (1979).
- [33] E. H. Lieb and J. P. Solovej, Acta Math. **212**, 379 (2014).
- [34] R. Gilmore, S. Kais, and R. D. Levine, Phys. Rev. A **34**, 2442 (1986).
- [35] P. Cejnar and P. Stránský, Phys. Rev. E **78**, 031130 (2008).
- [36] C. Emary, N. Lambert, and T. Brandes, Phys. Rev. A **71**, 062302 (2005).
- [37] H. Lipkin, N. Meshkov, and A. Glick, Nucl. Phys. **62**, 188 (1965).
- [38] P. Jurcevic et al., Nature **511**, 202 (2014).
- [39] P. Richerme et al., Nature **511**, 198 (2014).
- [40] R. Gilmore and D. H. Feng, Nucl. Phys. A **301**, 189 (1978).
- [41] R. Gilmore and D. H. Feng, Phys. Lett. B **76**, 26 (1978).
- [42] R. H. Dicke, Phys. Rev. **93**, 99 (1954).
- [43] B. M. Garraway, Phil. Trans. R. Soc. A **369**, 1137 (2011).
- [44] O. Castaños, E. Nahmad-Achar, R. López-Peña, and J. G. Hirsch, Phys. Rev. A **83**, 051601 (2011).

- [45] O. Castaños, E. Nahmad-Achar, R. López-Peña, and J. G. Hirsch, Phys. Rev. A **84**, 013819 (2011).
- [46] P. Nataf and C. Ciuti, Nat. Comm. **1**, 72 (2010).
- [47] C. Emary and T. Brandes, Phys. Rev. Lett. **90**, 044101 (2003).
- [48] C. Emary and T. Brandes, Phys. Rev. E **67**, 066203 (2003).
- [49] K. Baumann, C. Guerlin, F. Brennecke, and T. Esslinger, Nature **464**, 1301 (2010).
- [50] F. Iachello and A. Arima, *The Interacting Boson Model* (Cambridge University Press, Cambridge, 1987).
- [51] J. Vidal, J. M. Arias, J. Dukelsky, and J. E. García-Ramos, Phys. Rev. C **73**, 054305 (2006).
- [52] F. Iachello, Chem. Phys. Lett. **78**, 581 (1981).
- [53] F. Iachello and S. Oss, J. Chem. Phys. **104**, 6956 (1996).
- [54] D. Larese, F. Pérez-Bernal, and F. Iachello, J. Molec. Struct. **1051**, 310 (2013).
- [55] M. Caprio, P. Cejnar, and F. Iachello, Ann. Phys. **323**, 1106 (2008).
- [56] F. Pérez-Bernal and F. Iachello, Phys. Rev. A **77**, 032115 (2008).
- [57] K. Hepp and E. H. Lieb, Ann. Phys. **76**, 360 (1973).
- [58] Y. K. Wang and F. T. Hioe, Phys. Rev. A **7**, 831 (1973).
- [59] O. Castaños, E. Nahmad-Achar, R. López-Peña, and J. G. Hirsch, Phys. Rev. A **86**, 023814 (2012).
- [60] M. A. Bastarrachea-Magnani et al. (2015), arXiv quant-ph, 1509.05918.
- [61] S. Dusuel and J. Vidal, Phys. Rev. Lett. **93**, 237204 (2004).
- [62] W. D. Heiss, F. G. Scholtz, and H. B. Geyer, J. Phys. A: Math. Gen. **38**, 1843 (2005).
- [63] F. Leyvraz and W. D. Heiss, Phys. Rev. Lett. **95**, 050402 (2005).
- [64] O. Castaños, R. López-Peña, J. G. Hirsch, and E. López-Moreno, Phys. Rev. B **72**, 012406 (2005).
- [65] O. Castaños, R. López-Peña, J. G. Hirsch, and E. López-Moreno, Phys. Rev. B **74**, 104118 (2006).
- [66] D. H. Feng, R. Gilmore, and S. R. Deans, Phys. Rev. C **23**, 1254 (1981).
- [67] E. López-Moreno and O. Castaños, Phys. Rev. C **54**, 2374 (1996).
- [68] F. Iachello, N. V. Zamfir, and R. F. Casten, Phys. Rev. Lett. **81**, 1191 (1998).
- [69] J. Jolie et al., Phys. Rev. Lett. **89**, 182502 (2002).
- [70] J. M. Arias, J. Dukelsky, and J. E. García-Ramos, Phys. Rev. Lett. **91**, 162502 (2003).

- [71] M. Calixto, R. del Real, and E. Romera, Phys. Rev. A **86**, 032508 (2012).
- [72] O. Castaños, R. Lopez-Peña, and V. Manko, J. Russ. Laser Res. **16**, 477 (1995).
- [73] O. Castaños and J. A. Lopez-Saldivar, in *SYMMETRIES IN SCIENCE XV* (2012), vol. 380 of *Journal of Physics Conference Series*, ISSN 1742-6588, International Symposium on Symmetries in Science XV, Bregenz, AUSTRIA, JUL 31-AUG 05, 2011.